

Article

Maternal Nutrient Restriction Confers Myocardial Remodeling in Association with Dampened Autophagy and Mitophagy in Adult Sheep Offspring

Wei Ge¹, Qiurong Wang^{2,3}, Jun Tao⁴, Stephen P. Ford^{5,†}, Wei Guo^{6,7}, Xiaoming Wang^{8,*} and Jun Ren^{2,3,*}

¹ Department of General Practice, Xijing Hospital, Air Force Medical University, Xi'an 710032, China

² Department of Cardiology, Zhongshan Hospital Fudan University, Shanghai Institute of Cardiovascular Diseases, Shanghai 200032, China

³ National Clinical Research Center for Interventional Medicine, Shanghai 200032, China

⁴ Department of Cardiovascular Surgery, Sun Yat-Sen Memorial Hospital, Sun Yat-Sen University, Guangzhou 510000, China

⁵ Center for the Study of Fetal Programming, University of Wyoming, Laramie, WY 82071, USA

⁶ Department of Animal and Dairy Sciences, University of Wisconsin-Madison, Madison, WI 53706, USA

⁷ Cardiovascular Research Center, School of Medicine and Public Health, University of Wisconsin-Madison, Madison, WI 53706, USA

⁸ Department of Geriatrics, Xijing Hospital, Air Force Medical University, Xi'an 710032, China

* Correspondence: xmwang@fmmu.edu.cn (X.W.); ren.jun@zs-hospital.sh.cn (J.R.)

† Deceased.

Received: 19 October 2023; Revised: 23 November 2023; Accepted: 24 November 2024; Published: 13 February 2025

Abstract: The “thrifty phenotype” resulted from maternal malnutrition is considered a vital predisposing factor for the etiology of metabolic anomalies in offspring. To unveil the underlying mechanisms of heart diseases consequential to maternal malnutrition, pregnant ewes were kept on a nutrient restricted (NR: 50%) or control diet (100%) from day 28 to 78 of gestation. The experimental diet was then switched to a normal nutrition diet regimen till lambing. At 6 years of age, cardiac structure and function were evaluated following a 12-week palatable diet in adult offspring from control and maternal NR groups, along with insulin signaling, autophagy, mitophagy and pro-inflammatory cytokines. Our results revealed that offspring from NR ewes displayed greater body, heart, and ventricular weights along with cardiomyocyte mechanical anomalies (poor cell shortening capacity, prolonged relengthening and intracellular Ca²⁺ clearance with a pronounced response in left ventricles), cardiac remodeling (enlarged cardiomyocyte size and interstitial fibrosis) and O₂⁻ accumulation. Proinflammatory cytokines including TLR4, TNF α and IL1 β were upregulated in right ventricles along with higher STAT3 in left ventricles with little changes in GLUT4 following maternal NR. Levels of autophagy and mitophagy were downregulated in both ventricles from NR offspring (LC3BII, Atg7, Parkin, FUNDC1 and BNIP3 with higher p62 and unchanged Beclin1). Maternal nutrient restriction also promoted serine phosphorylation of IRS1 and suppressed AMPK phosphorylation without affecting Akt phosphorylation in both ventricles. Phosphorylation of mTOR was elevated in left but not right ventricles from NR offspring. These findings collectively unveiled a predisposing role of maternal malnutrition in cardiac anomalies in adulthood, possibly related to regulation of phosphorylation of IRS1 and AMPK, proinflammatory cytokines, autophagy and mitophagy. Targeting autophagy/mitophagy, IRS1 and AMPK such as using metformin and HM-chromanone may hold therapeutic promises in NR offspring with cardiac conditions.

Keywords: nutrient restriction; maternal; offspring; autophagy; mitophagy; insulin signaling



Copyright: © 2025 by the authors. This is an open access article under the terms and conditions of the Creative Commons Attribution (CC BY) license (<https://creativecommons.org/licenses/by/4.0/>).

Publisher's Note: Scilight stays neutral with regard to jurisdictional claims in published maps and institutional affiliations.

1. Introduction

Early-life environmental exposure is believed a major determining factor for pathogenesis of various chronic diseases later in life [1–7]. In particular, maternal or gestational nutrition status is a rather important driving force for fetal development, with maternal malnutrition being heavily correlated with organ abnormality and elevated disease susceptibility later on in life [2, 4, 6–9]. David Barker first coined the “thrifty phenotype” theory which helped to explain the connection between maternal nutrient insufficiency and fetal growth defect [10–12]. It is well perceived that maternal malnutrition during the first two trimesters is rather essential for increased prevalence of cardiovascular and metabolic anomalies in adult offsprings [10, 12–14]. For example, lambs from undernourished ewes were reported to display compromised health condition later in adulthood [15, 16], consistent with the rather important role for the first two trimesters of gestation in fetal development [16]. Nonetheless, little information is available with regards to the underlying regulatory machinery underscoring maternal malnutrition and offspring health issues.

Ample clinical and experimental findings have unveiled a key role for dampened insulin sensitivity in maternal malnutrition-evoked fetal growth retardation and offspring health defects in adulthood [2, 17]. Of note, fetal pancreatic β -cells confer an aberrant secretory modality following environmental nutrient deficiency during gestation [18]. Earlier findings from our group suggested involvement of insulin-like growth factor (IGF-1), a primary growth stimulating factor, in cardiac growth defect and remodeling following maternal malnutrition during the first two trimesters of gestation [19]. More recent evidence has suggested a role for profound inflammatory response in maternal malnutrition-evoked dysregulation of insulin signaling [20]. Measures such as coenzyme Q10 have been demonstrated to correct insulin signaling and inflammation prior to development of insulin resistance in adult offspring with poor maternal nutrition [21]. In an effort to better assess the effect of early gestational malnutrition on myocardial geometry and function, insulin signaling and inflammation in adult postnatal life, our present work was designed to examine myocardial function, geometry and morphology, inflammation as well as key elements of insulin signaling cascade encompassing insulin receptor substrate-1 (IRS1), and post-receptor signaling including Akt, AMP-dependent protein kinase (AMPK) and mammalian target of rapamycin (mTOR) [22]. Considering the recognized role of dysregulated autophagy/mitophagy as potential contributing factors in the governance of insulin sensitivity, inflammation and cardiac homeostasis [2, 23, 24], crucial signaling molecules in these cellular processes including toll-like receptor-4 (TLR-4), tumor necrosis factor α (TNF α), interleukin-1 β (IL-1 β), signal transducer and activator of transcription-3 (STAT3), microtubule-associated protein 1 light-chain 3 (LC3), p62, Beclin1, Atg7, Parkin, FUN14 domain containing 1 (FUNDC1), and Bcl-2/E1B-19 kDa interacting protein 3 (BNIP3) were examined in myocardium from offspring of control and nutrition-restricted ewes.

2. Materials and Methods

Experimental sheep: All animal procedures received approval from by our institutional Animal Care and Use Committee. Following four weeks of pregnancy, multiparous ewes were weighed and randomly divided into two groups. The control group received regular nutrient sufficient diet comprised of a pelleted beet pulp 79.7% total digestible nutrients (TDN), 93.5% dry matter (DM) and 10.0% crude protein—meeting 100% National Research Council (NRC) requirements including 100% mineral-vitamin mixture. The mineral-vitamin mixture comprises sodium triphosphate: 51.43%, potassium chloride: 47.62%, zinc oxide: 0.39%, cobalt acetate: 0.06% and ADE vitamin premix 0.50%, which was added to beet pulp to meet nutritional standard. The other group was nutrient-restricted (NR) (provided 50% NRC requirements including 50% mineral-vitamin mixture). Dams from both groups were maintained on respective diet regimen till 78 days of gestation (full term = ~150 days) before switching to 100% NRC requirements to term [19]. The rationale of choosing day 28–78 for nutrient restriction is based on the perceived notion that malnutrition during the first half of gestation overtly impairs fetal and placental growth and compromises the trajectory of fetal development. A 50% nutrient restriction during the first half of gestation has been shown to evoke compensatory growth of fetal ventricles [25]. At 6 years of age, female offspring of control and nutrient restricted ewes with comparable body weight were placed on an *ad libitum* highly palatable diet regimen for 12 weeks [26].

RNAseq analysis: Microarray expression dataset GSE124303 using adipose tissues from adult male mice with maternal nutrition restriction was downloaded from the Gene Expression Omnibus (GEO, <https://www.ncbi.nlm.nih.gov/geo/>) database. Nutrition restricted mice received 70% total diets (in weight) from embryonic day 6.5 till birth. Tissues were maintained in liquid nitrogen. Sequencing and polyA enrichment were used to create libraries. Differential expression analysis was performed on the training set using the “Deseq2” package for R software, with $|\logFC| > 2$ and adjusted p -value < 0.05 being the screening criteria to identify the differentially expressed genes. The R software packages “org.Mm.eg.db” and “clusterProfiler” were used to enrich the obtained differential genes in the Kyoto Encyclopedia of Genes and Genomes (KEGG) enrichment analyses. Adjust p -value < 0.05 was used as a filtering condition [27].

Isolation of cardiomyocytes and cell mechanical recording: Sheep ventricular tissues were perfused through a Krebs-Henseleit bicarbonate (KHB) buffer containing Liberase Blendzyme 4 (Hoffmann-La Roche Inc., Indianapolis, IN, USA) for 20 min. Rod-shaped cardiomyocytes with clear edges were chosen for functional study. Cardiomyocytes were electrically stimulated to contract at 0.5 Hz. Cell shortening and relengthening were captured using an IonOptix™ soft-edge device (IonOptix, Milton, MA, USA) including the following indices: peak shortening (PS), maximal velocities of shortening/relengthening ($\pm dL/dt$), time-to-PS (TPS), and time-to-90% relengthening (TR_{90}) was evaluated with [28–30].

Intracellular Ca^{2+} recording: For assessment of intracellular Ca^{2+} handling, cardiomyocytes were cultured with Fura-2/AM (0.5 μ M) for 15 min before fluorescence determination (excitation at 360 or 380 nm along with emissions between 480–520 nm). Resting and peak Fura-2 fluorescence intensity (FFI) and fluorescence decay were recorded [28,31].

Hematoxylin and eosin (H&E) staining: Following PBS rinsing, heart samples were incubated in 10% formalin for 24 h at room temperature before embedding the specimen in paraffin. Samples were sliced into 5- μ m sections prior to H&E staining. Cross-sectional areas were determined in cardiomyocytes using the NIH Image J (version 1.34S) software [32,33].

Masson trichrome staining: Ventricular tissues were sliced at the mid-ventricular level before fixation with formalin and preparation of 5- μ m Paraffin-embedded sections for Masson trichrome staining. Degree of interstitial fibrosis was presented as the light blue stained area normalized to the entire myocardial visualized field [32].

Intracellular superoxide ($O_2^{\cdot-}$): Myocardium was cultured with 5 μ M dihydroethidium (DHE) (Molecular Probes, Eugene, OR, USA) at 37 °C for 30 min and fluorescence intensity was captured using an Olympus microscope coupled with a digital camera followed by ImagePro data analysis [34].

Western blot analysis: Protein levels from sheep hearts were measured using the Bradford assay. Samples were isolated using SDS-polyacrylamide gels (10%) in a gel apparatus (Mini-PROTEAN II, Bio-Rad Laboratories, Inc, Hercules, CA) before switching to nitrocellulose membranes. Membranes were blocked with 5% milk in TBS-T, and were then incubated overnight at 4 °C with anti-TLR-4, anti-TNF- α , anti-IL-1 β , anti-GLUT4, anti-STAT3, anti-LC3B II, anti-p62, anti-Becclin1, anti-Atg7, anti-Parkin, anti-FUNDC1, anti-BNIP3, anti-IRS1, anti-phosphorylated IRS1 (pIRS1, Ser³⁰⁷), anti-AMPK, anti-phosphorylated AMPK (pAMPK, Thr¹⁷²), anti-Akt, anti-phosphorylated Akt (pAkt, Ser⁴⁷³), anti-mTOR, anti-phosphorylated mTOR (pmTOR, Ser²⁴⁴⁸), anti- α -tubulin and anti-GAPDH (both as loading control) antibodies. These antibodies all cross-reacted or reacted well with sheep myocardium. Following immunoblotting, films were scanned and gel band intensity was measured using a Bio-Rad Calibrated Densitometer [32,35].

Statistical analysis: All data are shown as Mean \pm SEM. Differences were determined using the student t-test with a p value < 0.05 being considered as statistically significant.

3. Results

3.1. Function Enrichment Analysis and General Features of Adult Offspring from Ewes Subjected to Nutrition Restriction

Function enrichment analysis of adipose tissues from maternal undernutrition and control groups demonstrated differentially expressed genes mainly associated with autophagy, insulin signaling, and inflammation pathways, suggesting involvement of autophagy, insulin signaling, and inflammation in the

progression of adipose tissue glucose tolerance (Figure 1a–c). Following the 12-week intake of a highly palatable diet, adult offspring of NR group exhibited a significantly greater body weight compared with the control group (Figure 1d). Average daily food intake was similar between control (0.64 ± 0.03 Kg/day) and NR (0.67 ± 0.05 Kg/day, $p > 0.05$) groups. Heart weight was overtly higher in NR offspring compared with the control group (Figure 1e). Moreover, maternal nutrient restriction significantly increased ventricular weights in both ventricles without affecting left or right ventricular wall thickness (Figure 1f,g).

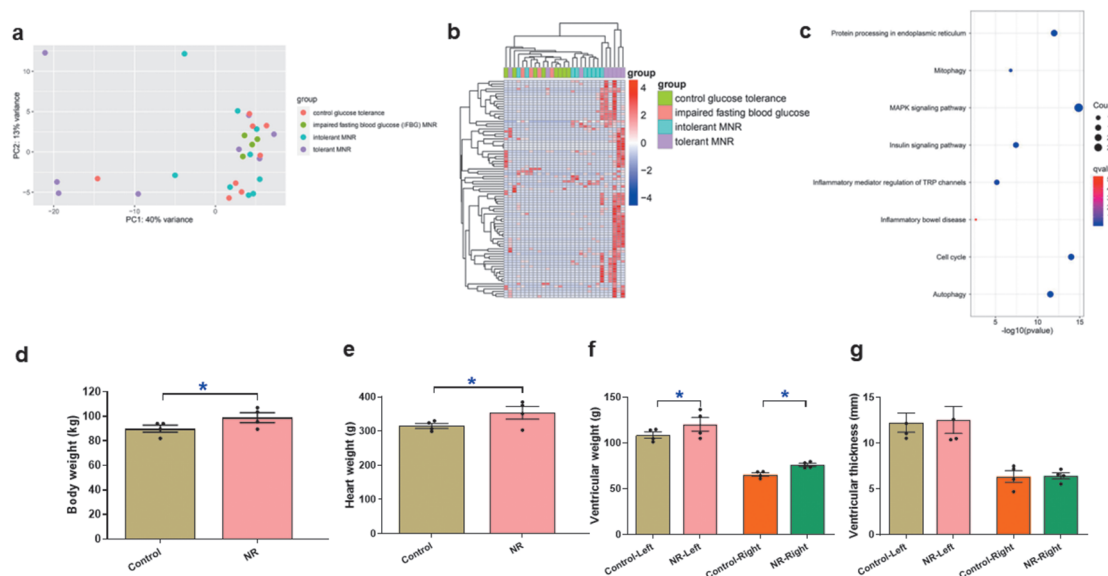


Figure 1. Heatmap and volcano plot for DEGs identified from GSE124303 dataset using adipose tissues from mice underwent maternal nutrient restriction (MNR). (a): PCA; (b): Heatmap exhibiting the top 100 upregulated and downregulated DEGs identified from GSE124303 dataset. Red and blue colors denote upregulation and downregulation, respectively; (c): KEGG pathway analysis of DEGs; (d–g): Body weight and whole heart, left or right ventricle from adult sheep offspring from control and nutrient restricted (NR) ewes. (d): Body weight; (e): Whole heart weight; (f): Left and right ventricular weight; and (g): Left and right ventricular wall thickness. Mean \pm SEM, $n = 4$; * $p < 0.05$ between indicated groups.

3.2. Cardiomyocyte Mechanical and Intracellular Ca^{2+} Properties in Adult Offspring with Maternal Nutrient Restriction

Assessment of individual cardiomyocyte mechanical property noted that maternal nutrient restriction overtly suppressed peak shortening (PS) in both ventricles and inhibited maximal velocities of shortening/relengthening (\pm dL/dt) along with prolonged time-to-90% relengthening (TR_{90}) in left but not right ventricles. Maternal nutrient restriction failed to alter resting cell length and time-to peak shortening (TPS) in either ventricle (Figure 2a–f). To decipher possible mechanism behind nutrient restriction-induced changes in cardiomyocyte contractile property, intracellular Ca^{2+} homeostasis was evaluated using Fura-2 fluorescent dye. Our results presented in Figure 2g–i indicated that maternal nutrient restriction overtly inhibited electrically-stimulated increase in intracellular Ca^{2+} (ΔFFI) in both ventricles and elongated intracellular Ca^{2+} clearance in left but not right ventricle without altering resting intracellular Ca^{2+} in either ventricle.

3.3. Morphological and Superoxide Properties in Hearts from Adult Offspring with Maternal Nutrition Restriction

H&E, Masson Trichrome and DHE staining techniques were used to discern myocardial morphological property and superoxide accumulation in hearts from control and maternal nutrient restriction offspring. Consistent with changes in cardiomyocyte properties, heart sections from both ventricles in adult offspring of nutrient restricted ewes exhibited overtly elevated cardiomyocyte cross-sectional size, interstitial fibrosis, and superoxide accumulation (Figure 3).

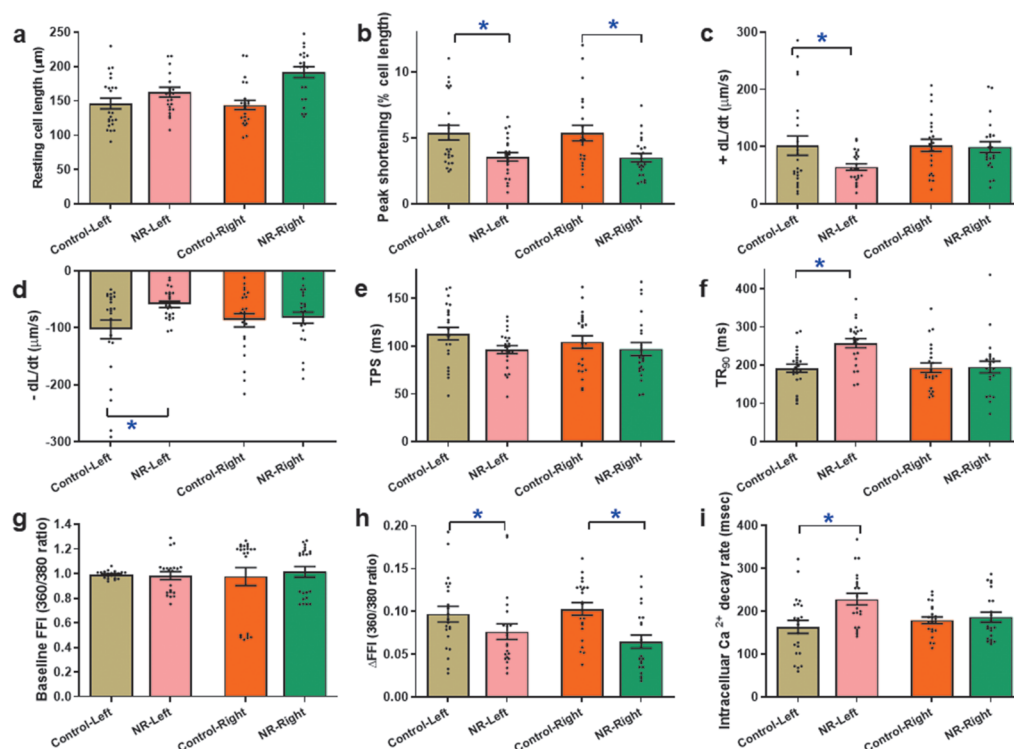


Figure 2. Cardiomyocyte contractile and intracellular Ca²⁺ properties of left ventricle (LV) or right ventricle (RV) from adult offspring of control and nutrient restricted (NR) ewes. (a): Resting cell length; (b): Peak shortening (PS, normalized to cell length); (c): Maximal velocity of shortening (+ dL/dt); (d): Maximal velocity of relengthening (−dL/dt); (e): Time-to-PS (TPS); (f): Time-to-90% relengthening (TR₉₀); (g): Resting intracellular Ca²⁺ Fura-2 fluorescence intensity (FFI); (h): Electrically-stimulated increase in intracellular Ca²⁺ (ΔFFI); and (i): Intracellular Ca²⁺ decay rate. Mean ± SEM, n = 22–23 cells per group, * p < 0.05 between indicated groups.

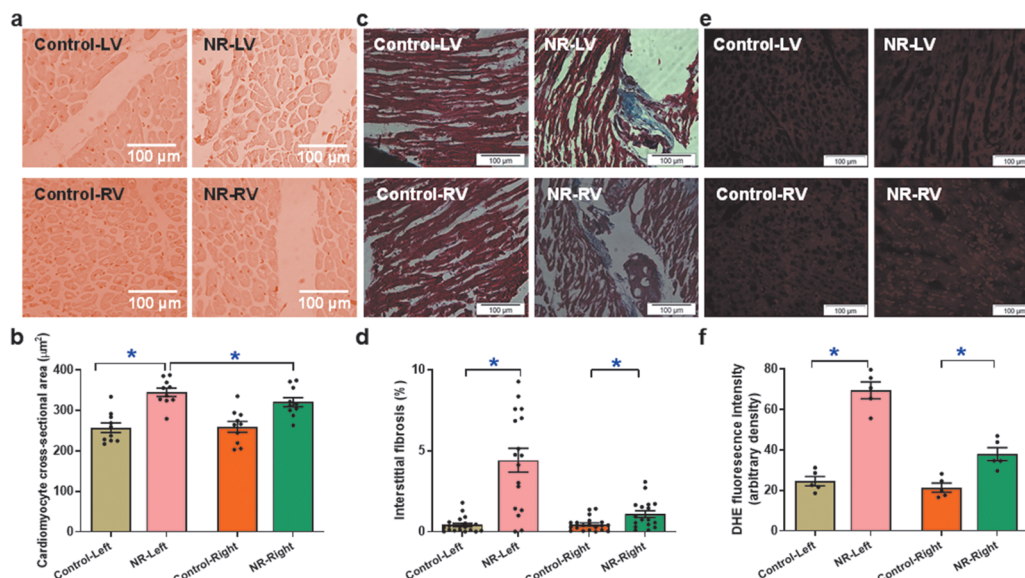


Figure 3. Hematoxylin and eosin (H&E) staining, Masson Trichrome staining and DHE staining of left ventricle (LV) or right ventricle (RV) from adult offspring of control and nutrient restricted (NR) ewes. (a): Representative micrographs of H&E staining (400×); (b): Quantitative assessment of cardiomyocyte cross-sectional area using H&E staining; (c): Representative micrographs of Masson Trichrome staining (400×); (d): Quantitative assessment of interstitial fibrosis using Masson Trichrome staining (light blue colored area normalized to total cardiac area); (e): Representative micrographs of DHE staining (400×); and f: Pooled data of myocardial superoxide accumulation using DHE staining. Mean ± SEM, n = 10–11 from panel b and d, n = 5 for panel (f). * p < 0.05 between indicated groups.

3.4. Proinflammatory Cytokines and Glucose Transporter in Hearts from Adult Offspring with Maternal Nutrient Restriction

Levels of proinflammatory and glucose transporter protein markers including TLR4, TNF α , IL1 β , GLUT4 and STAT3 were monitored in both ventricles of adult offspring from control and maternal nutrient restriction groups. Result shown in Figure 4 revealed upregulation of TLR4, TNF α and IL1 β in right but not left ventricles from adult offspring of maternal nutrient restriction group. Interestingly, level of STAT3 was upregulated in left but not right ventricles from offspring with maternal nutrient restriction. Level of GLUT4 remained unchanged in either ventricle following maternal nutrient restriction.

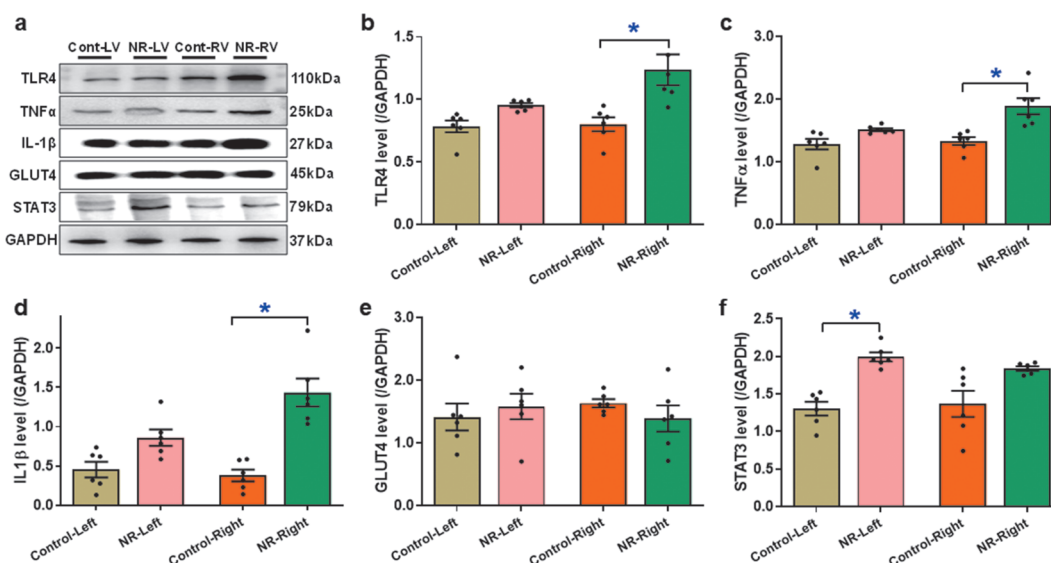


Figure 4. Levels of proinflammatory markers (TLR4, TNF α , IL1 β , STAT3) and glucose transport GLUT4 in left ventricle (LV) or right ventricle (RV) from adult offspring of control and nutrient restricted (NR) ewes. (a): Representative immunoblots depicting TLR4, TNF α , IL-1 β , GLUT4, and STAT3 (GAPDH as loading control) using specific antibodies; (b): TLR4 level; (c): TNF α level; (d): IL1 β level; (e): GLUT4 level; and (f): STAT3 level; Mean \pm SEM, n = 6 hearts per group, * $p < 0.05$ between indicated groups.

3.5. Autophagy and Mitophagy Protein Markers in Adult Offspring with Maternal Nutrition Restriction

Levels of autophagy and mitophagy protein markers including LC3B, p62, Beclin1, Atg7, Parkin, FUNDC1 and BNIP3 were assessed in hearts of adult offspring from ewes with or without maternal nutrient restriction. Results shown in Figure 5 revealed that compromised autophagy (LC3B, elevated p62, Atg7, Parkin, FUNDC1 and BNIP3) in both ventricles from maternal nutrient restriction groups (except a non-significant decline in LC3BII-to-LC3BI ratio in the right ventricle). Beclin1 levels remained unaltered in both ventricles in offspring following maternal nutrient restriction. These findings suggest possible association between dampened autophagy/mitophagy and myocardial geometric/functional anomalies following maternal nutrient restriction.

3.6. Levels of IRS1, AMPK, Akt and mTOR in Adult Offspring with Maternal Nutrition Restriction

Pan protein and phosphorylation of post-insulin receptor molecules including IRS1, AMPK, Akt and mTOR were scrutinized in hearts from adult offspring with or without maternal nutrient restriction. Absolute or normalized phosphorylation levels of IRS1 (Ser) and AMPK were overtly elevated and decreased, respectively, in both ventricles from maternal nutrient restriction group. Normalized phosphorylation of mTOR was enhanced in left but not right ventricle of offspring with maternal nutrient restriction (although absolute phosphorylation of mTOR remained unaltered in LV from maternal nutrient restriction group). Moreover, phosphorylation of the cellular fuel signal AMPK was unaffected in either ventricle by maternal nutrient restriction. Levels of pan protein expression of IRS1, AMPK, Akt and mTOR were not affected by maternal nutrient restriction in either ventricle (Figure 6).

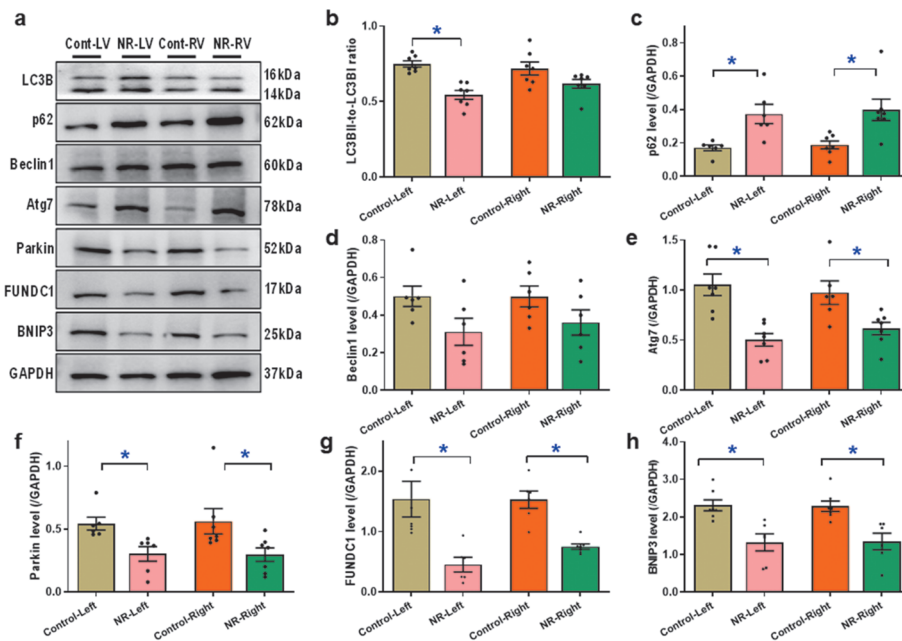


Figure 5. Levels of autophagy and mitophagy markers (LC3B, p62, Beclin1, Atg7, Parkin, FUNDC1 and BNIP3) in left ventricle (LV) or right ventricle (RV) from adult offspring of control and nutrient restricted (NR) ewes. (a): Representative immunoblots depicting LC3B, p62, Beclin1, Atg7, Parkin, FUNDC1 and BNIP3 (GAPDH as loading control) using specific antibodies; (b): LC3BII-to-LC3BI ratio; (c): p62 level; (d): Beclin1 level; (e): Atg7 level; (f): Parkin level; (g): FUNDC1 level; and (h): BNIP3 level; Mean \pm SEM, $n = 6-7$ hearts per group, * $p < 0.05$ between indicated groups.

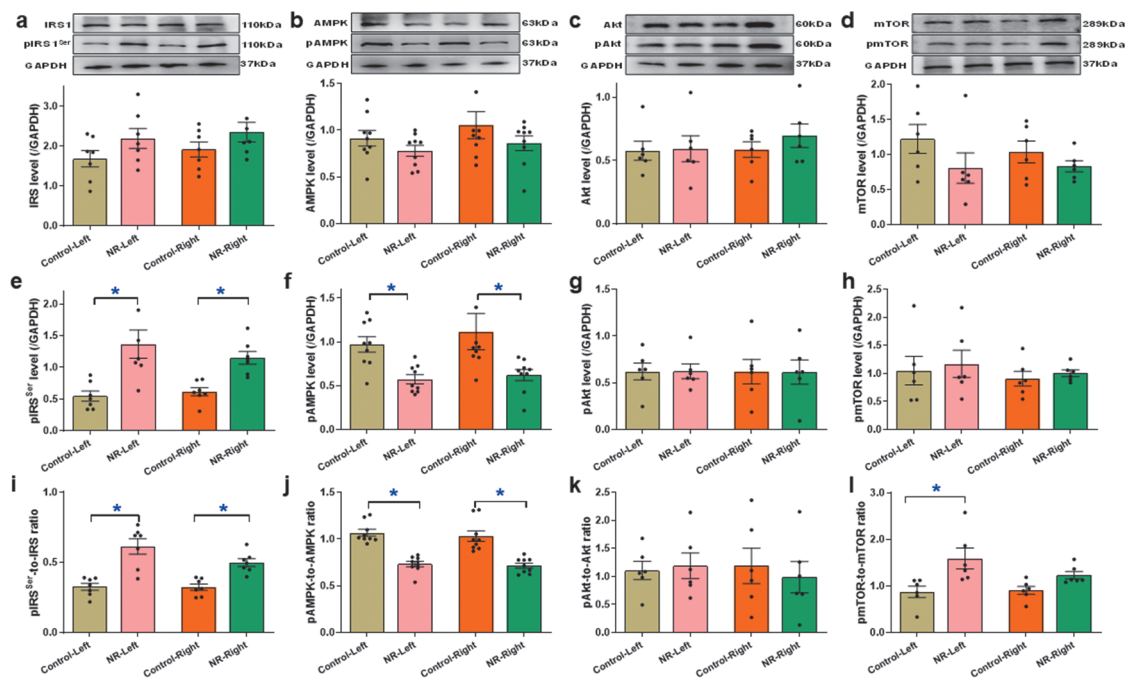


Figure 6. Pan protein and phosphorylation levels of IRS1, AMPK, Akt and mTOR in left ventricle (LV) or right ventricle (RV) from adult offspring of control and maternal nutrient restriction (NR) ewes. (a): Pan IRS1 level; (b): pan AMPK level; (c): Pan Akt level; (d): Pan mTOR level; (e): Serine phosphorylation of IRS1 (pIRS1, normalized to GAPDH); (f): Phosphorylated AMPK (pAMPK) normalized to GAPDH; (g): Phosphorylated Akt (pAkt) normalized to GAPDH; (h): Phosphorylated mTOR (pmTOR) normalized to GAPDH; (i): pIRS1 (Ser)-to-IRS1 ratio; (j): pAMPK-to-AMPK ratio; (k): pAkt-to-Akt ratio; and (l): pmTOR-to-mTOR ratio. Insets: Representative gel blots depicting levels of pan and phosphorylated IRS1, AMPK, Akt and mTOR (GAPDH as loading control) using specific antibodies; Mean \pm SEM, $n = 6-9$ hearts per group; * $p < 0.05$ between indicated groups.

4. Discussion

Salient findings from our work indicated that offspring underwent malnutrition during the early to mid-gestation are susceptible to development of cardiac anomalies, dysregulated insulin signaling, inflammation, oxidative stress and dampened autophagy/mitophagy later in their life. Prominent changes in cardiac geometry and function were demonstrated encompassing elevation in ventricular weights, cardiomyocyte size and interstitial fibrosis, compromised cardiac contractile and intracellular Ca^{2+} handling capacity in offspring underwent maternal malnutrition, which in large part coincide with findings from rodent model of maternal malnutrition [36,37]. Alteration in post-insulin receptor signaling was manifested as elevated serine phosphorylation of IRS1 (a negative regulator of insulin signaling) and dampened AMPK phosphorylation independent of regulation of Akt and GLUT4 in postnatal myocardium from sheep underwent maternal undernutrition. These findings favor a seemingly vital connection for dysregulated insulin signaling, autophagy/mitophagy, oxidative stress and proinflammatory responses in myocardial geometric and functional aberrations in adult offspring from ewes with maternal nutrient restriction.

Function enrichment analysis of adipose tissues from rodents identified genes associated with autophagy, insulin signaling, and inflammation pathways as the main differentially expressed genes associated with maternal undernutrition. This is supported by the overtly upregulated levels of proinflammatory cytokines such as TLR4, TNF α , IL1 β and STAT3 in both ventricles from adult offspring underwent maternal malnutrition. Earlier findings denoted a role for proinflammatory cytokines including TLR4, TNF α , IL1 β and STAT3 in the development of pathological cardiac hypertrophy [38,39], along with alleviation of pathological cardiac remodeling with antagonism of these cytokines [39,40]. Findings from our current study indicated that proinflammatory cytokines may play a potential contributing role in cardiac remodeling and dysfunction consequential to maternal malnutrition. Nonetheless, the precise mechanism with regards to how inflammation and cytokines are intertwined in maternal malnutrition-evoked cardiac anomalies warrants further research.

Insulin signaling is essential for cardiac growth, geometry, and function, ultimately cardiac homeostasis [22, 24]. Tyrosine phosphorylation of IRS1 fosters its interaction with cytoplasmic stakeholders to favor insulin signaling, while IRS1 serine phosphorylation is responsible for insulin resistance [22,41]. Findings from our work revealed elevated serine phosphorylation of IRS1 and depressed AMPK phosphorylation in postnatal myocardium (both ventricles) underwent nutrient restriction. Moreover, maternal malnutrition instigated a rise in mTOR phosphorylation in left but not right ventricles with little changes in Akt signaling and GLUT4. An anabolic role has been depicted for insulin signaling in myocardial homeostasis [22, 24]. Upon receptor binding, insulin evokes tyrosine phosphorylation of IRS1 to instigate a cadre of downstream signaling, including phosphatidylinositol-3 kinase/Akt cascade [22]. AMPK signaling, on the other hand, governs catabolism to inhibit cardiac growth [42]. In our hands, levels of serine phosphorylation of IRS1 were elevated, in favor of dampened insulin sensitivity in adult offspring from ewes with maternal nutrient restriction. Previous findings have indicated elevated and decreased serine phosphorylation and tyrosine phosphorylation, respectively, for IRS1 in the face of gestational diabetes [43,44], coinciding with our current findings.

AMPK phosphorylation was suppressed along with unaltered Akt signaling, in offspring hearts of maternal malnutrition group, suggesting possible contribution of dampened AMPK anabolic signaling to ventricular hypertrophy in both ventricles following maternal nutrient restriction. The Akt downstream signaling molecule mTOR belongs to phosphatidylinositol kinase-related kinase family [22], well known for its role in the regulation of cardiac hypertrophy and autophagy [24,45]. To our surprise, mTOR phosphorylation is upregulated in left but not right ventricle from offspring underwent maternal nutrient restriction. This finding appears to be in line with the pattern of LC3B response in both ventricles, suggesting a likely decisive role for mTOR in the regulation of autophagy in our current experimental setting. Nonetheless, with exception of LC3B and Beclin1, all other protein markers for autophagy and mitophagy exhibited a comparable response pattern in both ventricles following maternal nutrient restriction. Autophagy, an evolutionarily conserved cellular process for degradation/recycling of intracellular components, plays an important role in the face of nutrient scarcity such as maternal malnutrition [2,24,46]. Both autophagy and mitochondria-selective autophagy (a. k. a., mitophagy) help to sustain cardiac homeostasis under both

physiological and pathological conditions [24]. Our study reported, for the first time, presence of defective mitophagy (Parkin, FUNDC1 and BNIP3) in both ventricles from offspring following maternal nutrient restriction. Up-to-date, limited information is available with regards to correlations between maternal nutrition and mitophagy. Earlier finding from Rouschop and team suggested that perinatal obesogenic, high fat diet (overnutrition) stimulated mitophagy in lungs in female offspring [47], somewhat in line with our findings from a malnutrition perspective. Several experimental limitations exist for our study. First and foremost, the sample size was relatively small due to the difficulty in obtaining pregnant sheep model. Nonetheless, pregnancy in sheep offers advantage over rodent pregnancy to examine the influence of environmental or genetic changes of maternal milieu on postnatal health, as sheep mimics essential characters of pregnancy in human including length of pregnancy, monotocous and precocial pregnancy [48]. Compared with rodents, sheep myocardium shares many similarities to humans. For example, slow β -myosin heavy chain (β -MHC) isoform displays high similarity in sheep (~100%) and humans (>90–95%). Sheep exhibit a heart rate slightly higher than humans, much lower than rodents. The sarcoplasmic reticulum (SR) Ca^{2+} pump namely sarco(endo)plasmic Ca^{2+} -ATPase (SERCA) is responsible for 80% of Ca^{2+} clearance in diastole in sheep, reminiscent of the 76% contribution in humans. Both sheep and human hearts display a positive force-frequency relationship as opposed to the negative staircase in rodents [49,50]. Second, only female offspring was examined in this study, creating a possible bias for sex difference in postnatal myocardial health. Earlier evidence has noted presence of sex difference between male and female offspring underwent perinatal overnutrition [47]. Third, ingredients among maternal diets may also contribute, although remotely, to changes in heart health from offspring.

Drug development targeting serine or tyrosine phosphorylation of IRS1, AMPK activation, autophagy and mitophagy has exhibited great promises in cardiovascular medicine. For example, (E)-5-hydroxy-7-methoxy-3-(2'-hydroxybenzyl)-4-chromanone (HM-chromanone) isolated from *Portulaca oleracea* has shown high efficacy in attenuating inflammation and insulin resistance through suppression and stimulation of serine and tyrosine, respectively, phosphorylation of IRS1 [51]. Novel IRS1 serine phosphorylation stimulators (e.g., NT219) or IRS1 serine phosphorylation inhibitors (e.g., Coronarin A) have demonstrated utility in the management of cancer and metabolic diseases [52,53]. Of note, NT219 was reported to promote levels of certain molecular chaperones along with dampened autophagy [54], somewhat consistent with our current findings of compromised autophagy and dampened IRS1 signaling. Further study would be needed to elucidate their application in maternal or gestational nutrition derangement-associated comorbidities.

Metformin, a potent activator of AMPK, autophagy and mitophagy, has also exhibited benefit for various cardiovascular diseases associated with maternal malnutrition [55], coinciding with our current results for sheep model of maternal undernutrition. Nonetheless, most studies offered drug therapy such as metformin mothers during pregnancy [55,56]. Given the nature of large animal study for our current investigation, future study using more feasible rodent models is needed to test the efficacy of drugs targeting IRS1 phosphorylation, AMPK activation, autophagy and mitophagy in offspring with maternal malnutrition, in an “after-effect” modality.

In summary, findings from our study indicated that maternal nutrient restriction during the early to mid-gestation imposes pathological sequelae on cardiac geometry and function in adult offspring. Such changes in cardiac geometry and function appears to be related to elevated serine phosphorylation of IRS1 and dampened AMPK phosphorylation, evident oxidative stress, pro-inflammatory responses and compromised autophagy/mitophagy. Adequate maternal nutrition should be essential for fetal development, deficiency of which likely evokes fetal abnormalities and adulthood health issues, including heart and metabolic diseases [10, 14, 25]. These findings should shed some lights towards a better understanding with regards to the development of pathological cardiac remodeling and contractile anomalies in adult offspring underwent maternal malnutrition. Nonetheless, the precise interplay among autophagy/mitophagy defect, proinflammatory response and dysregulated cardiac homeostasis remains elusive and warrants further large-scale study.

5. Bullet Point Summary

- What is already known: Maternal malnutrition prompts myocardial dysfunction in association with

oxidative stress;

- What this study adds: Maternal undernutrition using sheep model triggers changes in cardiac geometric and functional defect in association with altered autophagy/mitophagy signaling;
- Clinical significance: We have revealed that maternal nutrition deficiency in sheep evokes cardiac dyshomeostasis via disturbed IRS1 and AMPK, proinflammatory cytokines, autophagy and mitophagy.

Author Contributions: W. G. (Wei Ge), Q. W., J. T., S. P. F. data collection and analysis; W. G. (Wei Guo): helpful discussion; X. W. and J. R. manuscript drafting, editing and supervision of the study. All authors have read and agreed to the published version of the manuscript.

Funding: Part of our present work was supported in part by the National Natural Science Foundation of China (Grant No. 82200483; 82270259) and the Natural Science Foundation of Guangdong Province (Grant No. 2023A1515011687).

Institutional Review Board Statement: No human subject or animals were involved.

Informed Consent Statement: Not applicable.

Data Availability Statement: Not applicable.

Conflicts of Interest: The authors declare that they have no conflict of interest.

References

1. Fan, X.; Turdi, S.; Ford, S.P.; et al. Influence of gestational overfeeding on cardiac morphometry and hypertrophic protein markers in fetal sheep. *J. Nutr. Biochem.* **2011**, *22*, 30–37.
2. Wang, L.; O’Kane, A. M.; Zhang, Y.; et al. Maternal obesity and offspring health: Adapting metabolic changes through autophagy and mitophagy. *Obes. Rev.* **2023**, *24*, e13567.
3. Wang, J.; Ma, H.; Tong, C.; et al. Overnutrition and maternal obesity in sheep pregnancy alter the JNK-IRS-1 signaling cascades and cardiac function in the fetal heart. *FASEB J.* **2010**, *24*, 2066–2076.
4. Dong, F.; Ford, S.P.; Nijland, M.J.; et al. Influence of maternal undernutrition and overfeeding on cardiac ciliary neurotrophic factor receptor and ventricular size in fetal sheep. *J. Nutr. Biochem.* **2008**, *19*, 409–414.
5. Kandadi, M. R.; Hua, Y.; Zhu, M.; et al. Influence of gestational overfeeding on myocardial proinflammatory mediators in fetal sheep heart. *J. Nutr. Biochem.* **2013**, *24*, 1982–1990.
6. Diniz, M.S.; Grilo, L.F.; Tocantins, C.; et al. Made in the Womb: Maternal Programming of Offspring Cardiovascular Function by an Obesogenic Womb. *Metabolites* **2023**, *13*, 845.
7. Zambrano, E.; Lomas-Soria, C.; Nathanielsz, P. W. Rodent studies of developmental programming and ageing mechanisms: Special issue: In utero and early life programming of ageing and disease. *Eur. J. Clin. Investig.* **2021**, *51*, e13631.
8. Roberts, J.M.; Heider, D.; Bergman, L.; et al. Vision for Improving Pregnancy Health: Innovation and the Future of Pregnancy Research. *Reprod. Sci.* **2022**, *29*, 2908–2920.
9. Huber, H. F.; Jenkins, S. L.; Li, C.; et al. Strength of nonhuman primate studies of developmental programming: Review of sample sizes, challenges, and steps for future work. *J. Dev. Orig. Health Dis.* **2020**, *11*, 297–306.
10. Bar, J.; Weiner, E.; Levy, M.; et al. The thrifty phenotype hypothesis: The association between ultrasound and Doppler studies in fetal growth restriction and the development of adult disease. *Am. J. Obstet. Gynecol. MFM* **2021**, *3*, 100473.
11. Vaag, A.A.; Grunnet, L.G.; et al. The thrifty phenotype hypothesis revisited. *Diabetologia* **2012**, *55*, 2085–2088.
12. Hales, C.N.; Barker, D.J. The thrifty phenotype hypothesis. *Br. Med. Bull.* **2001**, *60*, 5–20.
13. Godfrey, K.; Robinson, S. Maternal nutrition, placental growth and fetal programming. *Proc. Nutr. Soc.* **1998**, *57*, 105–111.
14. Dong, M.; Zheng, Q.; Ford, S.P.; et al. Maternal obesity, lipotoxicity and cardiovascular diseases in offspring. *J. Mol. Cell Cardiol.* **2013**, *55*, 111–116.
15. Barker, D.J. Coronary heart disease: A disorder of growth. *Horm. Res.* **2003**, *59* (Suppl. 1), 35–41.
16. Barker, D.J.; Gelow, J.; Thornburg, K.; et al. The early origins of chronic heart failure: Impaired placental growth and initiation of insulin resistance in childhood. *Eur. J. Heart Fail.* **2010**, *12*, 819–825.
17. Gupta, M.B.; Jansson, T. Novel roles of mechanistic target of rapamycin signaling in regulating fetal growth. *Biol. Reprod.* **2019**, *100*, 872–884.
18. Green, A. S.; Rozance, P. J.; Limesand, S. W. Consequences of a compromised intrauterine environment on islet function. *J. Endocrinol.* **2010**, *205*, 211–224.
19. Dong, F.; Ford, S.P.; Fang, C.X.; et al. Maternal nutrient restriction during early to mid gestation up-regulates cardiac insulin-like growth factor (IGF) receptors associated with enlarged ventricular size in fetal sheep. *Growth Horm. IGF Res.* **2005**, *15*, 291–299.
20. Tarry-Adkins, J. L.; Aiken, C. E.; Ashmore, T. J.; et al. Insulin-signalling dysregulation and inflammation is programmed trans-generationally in a female rat model of poor maternal nutrition. *Sci. Rep.* **2018**, *8*, 4014.
21. Tarry-Adkins, J. L.; Fernandez-Twinn, D. S.; Madsen, R.; et al. Coenzyme Q10 Prevents Insulin Signaling Dysregulation and Inflammation Prior to Development of Insulin Resistance in Male Offspring of a Rat Model of Poor Maternal Nutrition and Accelerated Postnatal Growth. *Endocrinology* **2015**, *156*, 3528–3537.

22. Ren, J.; Anversa, P. The insulin-like growth factor I system: Physiological and pathophysiological implication in cardiovascular diseases associated with metabolic syndrome. *Biochem. Pharmacol.* **2015**, *93*, 409–417.
23. Ajoobalady, A.; Chiong, M.; Lavandero, S.; et al. Mitophagy in cardiovascular diseases: Molecular mechanisms, pathogenesis, and treatment. *Trends Mol. Med.* **2022**, *28*, 836–849.
24. Zhang, Y.; Whaley-Connell, A. T.; Sowers, J. R.; et al. Autophagy as an emerging target in cardiorenal metabolic disease: From pathophysiology to management. *Pharmacol. Ther.* **2018**, *191*, 1–22.
25. Han, H.C.; Austin, K.J.; Nathanielsz, P.W.; et al. Maternal nutrient restriction alters gene expression in the ovine fetal heart. *J. Physiol.* **2004**, *558*, 111–121.
26. George, L. A.; Zhang, L.; Tuersunjiang, N.; et al. Early maternal undernutrition programs increased feed intake, altered glucose metabolism and insulin secretion, and liver function in aged female offspring. *Am. J. Physiol. Regul. Integr. Comp. Physiol.* **2012**, *302*, R795–R804.
27. Peng, H.; Zhang, J.; Zhang, Z.; et al. Cardiac-specific overexpression of catalase attenuates lipopolysaccharide-induced cardiac anomalies through reconciliation of autophagy and ferroptosis. *Life Sci.* **2023**, *328*, 121821.
28. Li, Q.; Wu, S.; Li, S. Y.; et al. Cardiac-specific overexpression of insulin-like growth factor 1 attenuates aging-associated cardiac diastolic contractile dysfunction and protein damage. *Am. J. Physiol. Heart Circ. Physiol.* **2007**, *292*, H1398–H1403.
29. Ren, J.; Wold, L. E. Measurement of Cardiac Mechanical Function in Isolated Ventricular Myocytes from Rats and Mice by Computerized Video-Based Imaging. *Biol. Proced. Online* **2001**, *3*, 43–53.
30. Wang, Q.; Zhu, C.; Sun, M.; et al. Maternal obesity impairs fetal cardiomyocyte contractile function in sheep. *FASEB J.* **2019**, *33*, 2587–2598.
31. Doser, T.A.; Turdi, S.; Thomas, D.P.; et al. Transgenic overexpression of aldehyde dehydrogenase-2 rescues chronic alcohol intake-induced myocardial hypertrophy and contractile dysfunction. *Circulation* **2009**, *119*, 1941–1949.
32. Ge, W.; Hu, N.; George, L. A.; et al. Maternal nutrient restriction predisposes ventricular remodeling in adult sheep offspring. *J. Nutr. Biochem.* **2013**, *24*, 1258–1265.
33. Sun, A.; Cheng, Y.; Zhang, Y.; et al. Aldehyde dehydrogenase 2 ameliorates doxorubicin-induced myocardial dysfunction through detoxification of 4-HNE and suppression of autophagy. *J. Mol. Cell Cardiol.* **2014**, *71*, 92–104.
34. Turdi, S.; Han, X.; Huff, A. F.; et al. Cardiac-specific overexpression of catalase attenuates lipopolysaccharide-induced myocardial contractile dysfunction: Role of autophagy. *Free Radic. Biol. Med.* **2012**, *53*, 1327–1338.
35. Ma, H.; Li, J.; Gao, F.; et al. Aldehyde dehydrogenase 2 ameliorates acute cardiac toxicity of ethanol: Role of protein phosphatase and forkhead transcription factor. *J. Am. Coll. Cardiol.* **2009**, *54*, 2187–2196.
36. Masoumy, E. P.; Sawyer, A. A.; Sharma, S.; et al. The lifelong impact of fetal growth restriction on cardiac development. *Pediatr. Res.* **2018**, *84*, 537–544.
37. Harvey, T.J.; Murphy, R.M.; Morrison, J.L.; et al. Maternal Nutrient Restriction Alters Ca²⁺ Handling Properties and Contractile Function of Isolated Left Ventricle Bundles in Male But Not Female Juvenile Rats. *PLoS ONE* **2015**, *10*, e0138388.
38. Molaei, A.; Molaei, E.; Hayes, A. W.; et al. Mas receptor: A potential strategy in the management of ischemic cardiovascular diseases. *Cell Cycle* **2023**, *22*, 1654–1674.
39. Lillo, R.; Graziani, F.; Franceschi, F.; et al. Inflammation across the spectrum of hypertrophic cardiac phenotypes. *Heart Fail. Rev.* **2023**, *28*, 1065–1075.
40. Sriramula, S.; Haque, M.; Majid, D.S.; et al. Involvement of tumor necrosis factor-alpha in angiotensin II-mediated effects on salt appetite, hypertension, and cardiac hypertrophy. *Hypertension* **2008**, *51*, 1345–1351.
41. Copps, K.D.; Hancer, N.J.; Opore-Ado, L.; et al. Irs1 serine 307 promotes insulin sensitivity in mice. *Cell Metab.* **2010**, *11*, 84–92.
42. Sanz, R. L.; Inerra, F.; Garcia Menendez, S.; et al. Metabolic Syndrome and Cardiac Remodeling Due to Mitochondrial Oxidative Stress Involving Gliflozins and Sirtuins. *Curr. Hypertens. Rep.* **2023**, *25*, 91–106.
43. Shao, J.; Yamashita, H.; Qiao, L.; et al. Phosphatidylinositol 3-kinase redistribution is associated with skeletal muscle insulin resistance in gestational diabetes mellitus. *Diabetes* **2002**, *51*, 19–29.
44. Shao, J.; Catalano, P. M.; Yamashita, H.; et al. Decreased insulin receptor tyrosine kinase activity plasma cell membrane glycoprotein-1 overexpression in skeletal muscle from obese women with gestational diabetes mellitus (GDM): Evidence for increased serine/threonine phosphorylation in pregnancy and GDM. *Diabetes* **2000**, *49*, 603–610.
45. Nair, S.; Ren, J. Autophagy and cardiovascular aging: Lesson learned from rapamycin. *Cell Cycle* **2012**, *11*, 2092–2099.
46. Ren, J.; Wu, N.N.; Wang, S.; et al. Obesity cardiomyopathy: Evidence, mechanisms, and therapeutic implications. *Physiol. Rev.* **2021**, *101*, 1745–1807.
47. Rouschop, S.H.; Snow, S.J.; Kodavanti, U.P.; et al. Perinatal High-Fat Diet Influences Ozone-Induced Responses on Pulmonary Oxidant Status and the Molecular Control of Mitophagy in Female Rat Offspring. *Int. J. Mol. Sci.* **2021**, *22*, 7551.
48. Nathanielsz, P. W. A time to be born: Implications of animal studies in maternal-fetal medicine. *Birth* **1994**, *21*, 163–169.
49. Milani-Nejad, N.; Janssen, P.M. Small and large animal models in cardiac contraction research: Advantages and disadvantages. *Pharmacol. Ther.* **2014**, *141*, 235–249.
50. Davidoff, A.J.; Ren, J. Low insulin and high glucose induce abnormal relaxation in cultured adult rat ventricular myocytes. *Am. J. Physiol.* **1997**, *272*, H159–H167.

51. Park, J.E.; Kang, E.; Han, J.S. HM-chromanone attenuates TNF-alpha-mediated inflammation and insulin resistance by controlling JNK activation and NF-kappaB pathway in 3T3-L1 adipocytes. *Eur. J. Pharmacol.* **2022**, *921*, 174884.
52. Jacob Berger, A.; Gigi, E.; Kupersmidt, L.; et al. IRS1 phosphorylation underlies the non-stochastic probability of cancer cells to persist during EGFR inhibition therapy. *Nat. Cancer* **2021**, *2*, 1055–1070.
53. Huang, S.L.; Xie, W.; Ye, Y.L.; et al. Coronarin A modulated hepatic glycogen synthesis and gluconeogenesis via inhibiting mTORC1/S6K1 signaling and ameliorated glucose homeostasis of diabetic mice. *Acta Pharmacol. Sin.* **2023**, *44*, 596–609.
54. Moll, L.; Ben-Gedalya, T.; Reuveni, H.; et al. The inhibition of IGF-1 signaling promotes proteostasis by enhancing protein aggregation and deposition. *FASEB J.* **2016**, *30*, 1656–1669.
55. Garcia-Contreras, C.; Vazquez-Gomez, M.; Pesantez-Pacheco, J.L.; et al. Maternal Metformin Treatment Improves Developmental and Metabolic Traits of IUGR Fetuses. *Biomolecules* **2019**, *9*, 166.
56. Gatford, K. L.; Houda, C. M.; Lu, Z. X.; et al. Vitamin B12 and homocysteine status during pregnancy in the metformin in gestational diabetes trial: Responses to maternal metformin compared with insulin treatment. *Diabetes Obes. Metab.* **2013**, *15*, 660–667.